



## Rock mass classification of Eocene karstic limestone in New Galala City, Northern Galala Plateau, Gulf of Suez, Egypt

Amr Gouda Abdel-Gawad<sup>(1)\*</sup>, Laila Fayed<sup>(1)</sup>, Mohamed Abdel-Wahed<sup>(1)</sup> and

Hesham Helmy<sup>(2)</sup>

<sup>(1)</sup> Geology Department, Faculty of Science, Cairo University, Cairo, Egypt.

<sup>(2)</sup> Structural Engineering Department, Faculty of Engineering, Ain Shams University, Cairo, Egypt.

**T**HE EGYPTIAN Government is aiming to construct new urbanization development projects in order to expand beyond the old Capital; Galala city is one of the greatest new cities projects. The project location is sited on Karstic limestone that necessitates detailed and careful geological and geotechnical studies. The present research is focused on detailed field investigation, rock mass classification, evaluation of rock quality and stability for foundation of the new Galala City and the new highway crossing the karstic Lower Eocene limestone capping the Northern Galala Plateau.

Detailed joint characterization is done through careful site investigations to evaluate the different parameters of discontinuities found in five stations. Rock Mass Rating (RMR) as a measure of the strength and rock mass deformation properties is determined to define the limitations in the rock mass and the unstable areas based on study of in-situ strength, groundwater condition, and joint condition measurements. Slope Mass Rating (SMR) is evaluated depending upon the RMR value added to factors including dip and dip direction of slope in relation to the different joint sets and also excavation method in the different study locations and the effect of geologic structures include fractures, joints, faults and damage zones. Kinematic analysis is performed to detect the potentiality of the different types of failure modes in the selected sites.

The study specifies good (Class II) to fair (Class III) in RMR and Normal rock quality and partly stable in SMR classification for the studied locations. Kinematic analysis indicates the possibility of planar, wedge and toppling failure in most locations, however, the most critical situation is found in two location; one along the asphaltic road and the other on a NW trending scarp limiting the city location from its norther border. The first location is considered safe for wedge failure with factor of safety higher the unity under static and dynamic conditions. The second location is unsafe for wedge failure with safety factor smaller than unity even under static condition.

The study indicates a good foundation for urbanizing a new city if the effect of human urban water factors on the foundation bedrock karstic limestone is taken into account. The presence of a scarp bounding the city location from its northeastern border represents a critical situation that must be taken in consideration.

**Keywords:** Rock Mass Rating, Slope Mass Rating, Kinematic Analysis, Eocene Karstified Limestone, Northern Galala Plateau, Rock Slope Stability.

\*Corresponding author: [agouda@sci.cu.edu.eg](mailto:agouda@sci.cu.edu.eg)

Received: 10/08/2022; Accepted: 20/09/2022;

DOI: 10.21608/EGJG.2022.154985.1022

©2022 National Information and Documentation Center (NIDOC)

## I. Introduction

The Galala new city is one of the greatest new cities under construction that the Egyptian Government has planned to expand beyond the old Capital. The project is located on the Northern Galala plateau occupying the coastal part of its second level that sits over 650 m a.s.l. at its highest elevation. The Northern Galala (El Galala El Bahariya) Plateau lies on the western coast of the Gulf of Suez between Ain Sokhna and Zafarana (Fig. 1). It is mainly covered with Eocene karstic limestone and constitutes the highest elevation in the Gulf of Suez region attaining an elevation over 1200 m a.s.l.

The city is considered as one of the biggest projects in Egypt. It will be an attractive city overlooking the Gulf of Suez from high levels and lies to the south of Ain El-Sokhna coastal touristic area. It occupies about 20 sq.km and will include several hotels, service and medical projects, King Abdullah University, and a new highway linking Qattamiya-Ain Sukhna road to Zafarana crossing the Galala Plateau.

The point of research is carefully chosen for the prime importance of the project in the governmental planning; to study the characteristics of the foundation bedrock, and the effect of the geological structures on the karstic limestone in the city location. The area under investigation lies between latitudes 29° 24' 28.5" N and 29° 35' 36" N and longitudes 32° 16' 09" E and 32° 27' 48" E (Fig. 1).

The engineering problems found in karst areas include the development of an irregular soil-bedrock contact, the formation of solution features as caves and sinkholes, and the weathering of the carbonate rock to a highly plastic residual soil (Adams and Lovell, 1984). The presence of faults can cause additional foundation problems by compressible gauge, altered wall rock, and offset groundwater levels, as well as highly fractured rock, which may also cause a marked reduction in safe-bearing pressures. Also, satisfactory rocks undergo appreciable deformation connected with the closing and sliding of joints (Abdel Wahed *et al.*, 2007).

The failure mechanisms as mentioned by Basahel *et al.* (2017), may be structurally controlled failure affected by different discontinuities orientations in relation to slope face orientation leading to structurally controlled failure (as Planar, Wedge, and Toppling failure) and non-structurally controlled failure which is influenced by groundwater effect, high weathering degree of outcrops, caving karstic features and dissolution. Ogila, *et al.*, 2021, studied the cliffs along the coastal highway between Ain-Sukhna and Zafarana cities. The slopes are considered stable under static conditions and their stability condition is highly reduced in water saturated conditions where the factor of safety is lower than unity.



Fig. 1. Location map of the study area.

Evaluation of mechanical and petrophysical properties of the karstic limestone became essential to avoid future risks in the construction of new urban cities built on limestones, also, the evaluation of the engineering and geomechanical properties of the bedrock is an important issue for designing the foundation types and for safe urban expansion (Abd El-Aal et al., 2017).

Construction of new cities on karstic limestone areas needs a detailed and careful site investigation and laboratory work. Rock mass classification helps in the evaluation of the rock quality of the foundation bedrocks and slope stability assessment is essential for the evaluation of road cuts and cliff edges.

Karstification in limestones constitutes a great problem facing the new Egyptian cities and newly constructed roads as mentioned in many studies; 15<sup>th</sup> May City (Mohammed et al., 2020), Beni-Suef El Gedida city (Abdel Wahed et al., 2007), El Minia El Gedida city (Abdeltawab and Ibrahim, 1991; Abdeltawab, 2013) and Sohag-Assiut highways (El-Haddad et al., 2021). Slope stability and rock collapse problems affected these locations. Buildings in these cities suffer progressively from engineering problems which are increased over the last 10 years like cracks, fissures, cavities, and tilting of buildings (Mohammed et al., 2020).

## II. Geological setting:

The exposed section of the Northern Galala area is considered as a pre-rift sequence, ranging in age from Late Paleozoic clastics to Early Eocene carbonates and dissected by basaltic dykes associated with Gulf of Suez rifting. Late Paleozoic and Mesozoic (Jurassic and Cretaceous) rocks are exposed on the rift shoulder as faulted blocks and separated by Permo- (?) Triassic continental red beds. Galala plateau is covered by Early Eocene nummulitic limestones where the study area is focused.

Three major dip domains are recognized in the Gulf of Suez which are separated by two accommodation zones marking the change in the regional dip. The Northern Galala block lies within the northern mega-half graben dip province. The northern mega-half graben of the Suez Rift has a SW dip with an average dip of the pre-rift rocks as 12°. The dip angles of the tilted blocks in the Suez Rift increase from NW to SE (Moustafa and Khalil, 2020).

The Gulf of Suez is bounded by NW-SE oriented major normal faults. Four major fault trends dominate the Suez rift have been recognized by Moustafa and Khalil (1995, 2020). The

NW-SE clysmic trend is the dominant fault system and constitutes the main orientation of the extensional faults in the Gulf. The North-Northeast Aqaba trend (N 10°-20°E) is the second major fault orientation. It is found predominantly in the southern parts of Gulf where it is affected by the Gulf of Aqaba-Dead Sea transfer system. These faults commonly form the linkages between the northwest rift faults producing the characteristic rhomboidal fault pattern seen at the rift border fault systems. The Duwi trend and cross fault trend are minor cross fault orientations as they are influenced by basement grains. The Duwi trend and cross-fault trend are oriented 100° to 120° and 040° to 060°, respectively.

Two structural phases were detected by Moustafa and Khalil (1995, 2020) in the Gulf of Suez region. Late Cretaceous to Recent Tethyan convergence of the African and Eurasian Plates that affected Egypt by compressive stress started during the Late Cretaceous time. In the Late Cretaceous phase of deformation, Syrian Arc folds with NE-SW oriented axes were formed as basin inversion of the Jurassic extensional basins/sub-basins in northern Egypt as a result of convergence between Africa and Eurasia and the closure of the Neotethys. The second phase is the Neogene rifting (late Oligocene - early Miocene phase); NNW-SSE normal faults were formed as a result of the opening of the Suez Rift. The carbonate platform in the study area is formed due to the initial topography controlled by the tectonic uplift of the Northern Galala/Wadi Araba Syrian Arc structure (Scheibner et al. 2001).

Saada (2016) applied the magnetic method to estimate the depth of basement rocks in the Galala El Bahariya Plateau. The depth estimation was applied using different techniques and found to be ranging from about 240 to 4340m. Moreover, these techniques indicate that the area is highly affected by the Gulf of Suez rifting system and the older E-W trend that is related to the Tethyan or Mediterranean trend.

Moreover, Abdelazeem et al. (2019) studied the integration of magnetic and stratigraphic data to delineate the subsurface features beneath the New Galala City, to avoid possible geological hazards. The observed palaeokarst surfaces, fissures, caves, sinkholes, and fault zones within carbonate rocks may cause some geological hazards in the study area. The study estimated both structural trends and source depths. The source depths range from 500 m to 4000 m, which results from the Precambrian basement complex.

However, the trends of encountered structural elements are mainly NE–SW, NW–SE, NNW–SSE, and E–W directions.

Detailed fieldwork and geological mapping of the study area (Fig.2) indicate two main trends of normal faults affecting the distribution of the exposed rock units of NW-SE and E-W to ENE-WSW directions. The first is younger and related to the Red Sea tectonics, while the second is older and responsible for the uplift of El Galala fault block and control the architecture of Wadi Ara-

ba to the south of the mapped area. The E-W to ENE-WSW faults are only recorded at the northern parts of the study area. Both fault trends are characterized by tilting of downthrown blocks and the presence of a considerable damage zone along their planes (Fig. 3.a). Shale smearing and dragging along fault planes cutting across the Cretaceous rocks are a common feature in the southeastern parts of the study area (Fig. 3.b). The joint trends measured in five locations within the area indicate four main trends; ENE, NNW, NNE, and WNW, in decreasing order of abundance (Fig. 4).

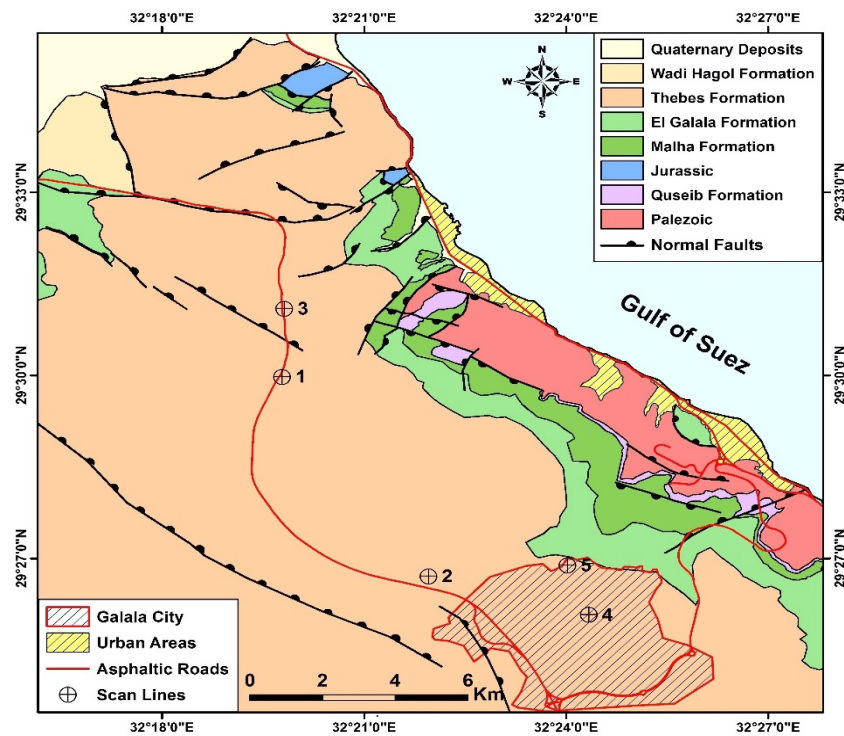


Fig. 2. Geological map of the study area (modified after Abdallah and Adindani, 1963, Boukhary *et al.*, 2009, CONOCO, 1987, Hammad and Abdel Khalik, 2015).

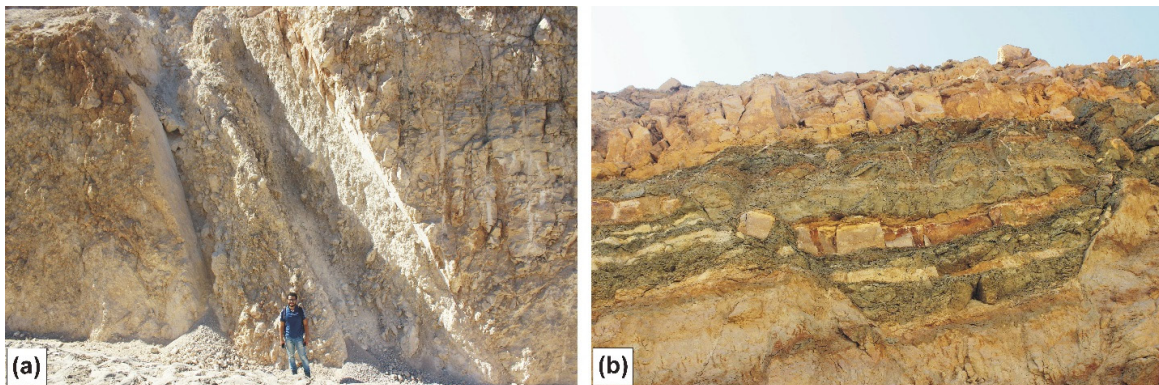


Fig. 3. a) Damage zone along NW normal fault cutting across the highway in the northern part of the study area. b) Dragging and shale smearing along NW normal fault in the Cretaceous rocks at the southeastern part of the area.

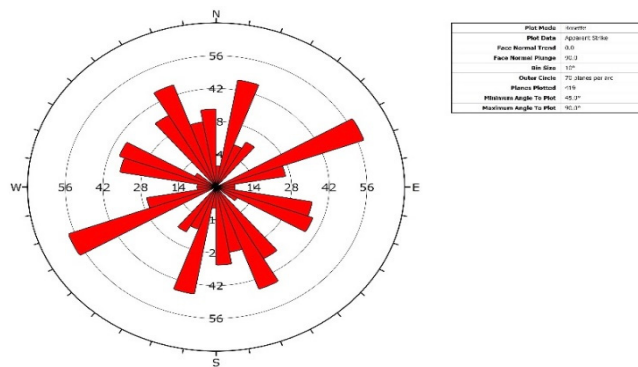


Fig. 4. Rose diagram representing the main joint trends in the study area (419 planes).

### III. Generalized Stratigraphy for the study area:

The sedimentary succession of the Northern Galala (Fig.2) could be subdivided into lower clastic sequence ranges in age from Late Carboniferous to Albian, middle marine Upper Cretaceous sequence, and upper carbonates Paleocene to Lower Eocene sequence. These sequences are briefly discussed as follows.

#### Lower Clastic sequence

**Paleozoic rocks:** The Upper Palaeozoic rocks cropping out on the western side of the Gulf of Suez of Egypt were studied by many authors, among them Abdallah and Adindani (1963), Bandel and Kuss (1987), Darwish (1992). They are exposed as faulted blocks along the coastal strip of the Gulf of Suez. They are mainly clastic facies composed of pebbly, gravelly sandstones with chocolate clay, crinoidal limestone, and fossiliferous marls inter-beds.

The **Permo-? Triassic Qiseib Formation** (Abdallah and Adindani, 1963) unconformably overlies the Upper Palaeozoic. Lithologically, is composed of sandstone, siltstone and mudstone interbedded with carbonate intercalations. It represents fluvial sequence braided stream deposits (Wanas and Soliman, 2018).

**Jurassic rocks** in the Northern Galala exposed in two spots, at Khashm El Galala (200m thick) and Ras El Abd, which is Middle Jurassic (Bathonian) sandstones interbedded in the upper part with two limestone beds and unconformably underlay the Lower Cretaceous Malha Formation (El Qot et al., 2009)

The exposed **Cretaceous rocks** are controlled by both Syrian arc and rift tectonics. They are started with Lower Cretaceous fluvial sandstones

Malha Formation which is unconformably overlain by the Cenomanian marine green shales and marls of the Galala Formation.

**Malha Formation** of Albian Cretaceous age (Abdallah and Adindani, 1963; Abdallah et al., 1963), is mainly composed of fine-grained white to pale brown fine to coarse sandstones occasionally pebbly, and cross-bedded with kaolinite clays.

#### Marine Upper Cretaceous sequence

The marine upper Cretaceous started with **Galala Formation** (Abdallah and Adindani, 1963; Abdallah et al., 1963). It is formed from green glauconitic shales and yellow fossiliferous marls with thin limestones of Cenomanian - Early Turonian age, unconformably overlies the fluvio-marine Malha Formation. It measures about 80-120 m.

#### Carbonate sequence

**The Eocene rocks (Thebes Formation)** form a huge mass of dolomitic limestone of Ypresian and Early Lutetian age capping the Northern Galala Plateau. It constitutes the bedrock for Galala City and its roads. The thickness and facies development of the Lower Eocene were controlled by tectonic phases of the Syrian arc and regional uplift during the closing of the Neotethys (Keheila, 2000; Kuss et al., 2000). The maximum measured thickness of Lower Eocene ranges from 512m at wadi Umm Russeies (Boukhary et al., 2009) to 548.5 in wadi Naot sections. The Thebes Formation exposed in the study area is discussed as follows:

**Thebes Formation:** The Thebes Formation is classified into the lower, middle, and upper members by El Boukhary et al. (2009) based on lithology and fossil contents, summarized as follows:

**The Lower Member:** This member is composed of white to pale white limestone and marl to

marly limestone of yellowish-white color, slightly hard, with rare chert nodules in the upper part. The thickness of this horizon ranges from 25 to 40 m and increases towards the western side of the study area.

**The Middle Member:** This member is composed of a sequence of well-bedded, white, or cream limestone, with poorly lithified bands of chalky to marly limestone, rich in chert bands and nodules. It is also characterized by the cyclic presence of hard bands of limestone about 30–50 cm thick and is overlain by thinner (10–15 cm) soft bands of a chalky to marly limestone. The thickness of this member ranges from 50–90 m, increasing towards the west.

**The Upper member:** It is represented by massive white to snow white chalky limestone, and massive, hard to moderately hard nummulitic limestone. The nummulitic limestone member measures about 100 to 160 m at sections. (El Boukhary *et al.*, 2009).

**Miocene Hagul Formation:** Non-marine Miocene only found in the northwestern parts of the study area as a downthrown block of two intersecting faults (Fig. 2). Its age is late Miocene, and is represented by continental fluvial clastic facies. It is made up of dark yellow sandstones, gravels, and pebbly sandstones (Abdallah and Abd El Hady, 1966).

#### IV. Methodology

Five scan lines (stations) are carefully chosen for detailed field investigation (Fig. 2), where good vertical cuts are present, more discontinuities engaged with slope faces are found and critical relations are expected along the main road and city location.

Station numbers 1, 2, and 3 are located along the main asphaltic road leading to the city, where station 3 is close to a fault plane cutting across the road (Fig.2). Stations 4 and 5 are within the city location, where station 5 is located along a NNW trending steep scarp bounds the city at its N border (Figs. 2 & 5) and elevated by about 200 m from the wadi level.

All stations are studied by the scanline method for recording all data and measurements for appropriate site investigation (Batron, 1979). Data collection is performed using Brunton compass, GPS, and measuring tape.

Engineering rock mass classification systems have been widely used nowadays depending on rating and ranking systems for rock quality evaluation. The rock mass classification systems, particularly those established for rock slopes, were used to determine the stability of rock cuttings for the specified rock slopes. To do so, the Rock Mass Rating (RMR) must be established, as well as the kind of failure mechanism for jointed rock masses.

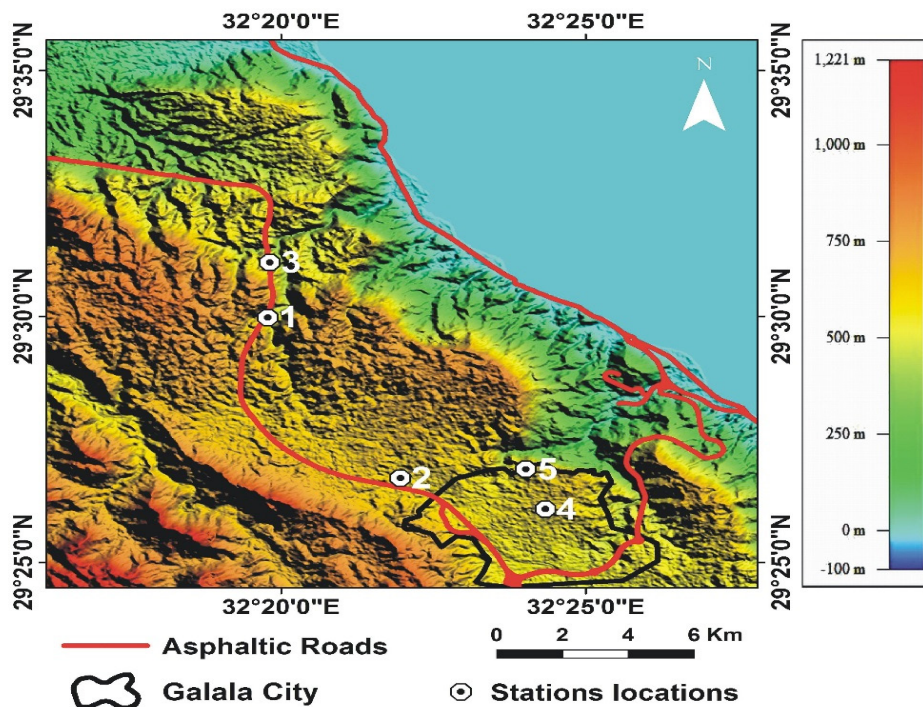


Fig. 5. Shaded relief model of the study area showing the location of new Galala city and studied stations.

In the present study, Rock Mass Rating (Bieniawski, 1973 and 1989) and Slope Mass Rating (Romana, 1985 and Romana et al. 2003, 2015) systems are applied to evaluate the rock quality and slope stability of the foundation bedrock of the city's location and surroundings. Kinematic analysis studies for probable failure types are done on the chosen stations to determine possible failure modes.

#### IV-1. Rock Mass Rating (RMR):

Bieniawski (1973 and 1989) suggested RMR basic system based on his experiences in shallow tunnels in sedimentary rocks. To determine the RMR basic value, the geotechnical data must be converted to numerical values (Singh and Goel, 2011), which reflect the ratings assigned to the input parameters based on proposed scheme tables for evaluation.

The following five parameters (representing causative factors) are evaluated for the rock exposures in the chosen locations:

1. Uniaxial compressive strength (UCS): is measured for 15 cylindrical core samples to represent the UCS of the rocks following ASTM D 2938 – 95 Standard Test Method for Unconfined Compressive Strength of Intact Rock Core Specimens. It is worth mentioning that, the North Galala plateau is occupied by one and the same rock unit (Thebes Formation limestones) that represents the foundation bedrock of the city location and the asphaltic road.
2. Rock quality designation (RQD) by Deere (1968): which is the total core samples count greater than 10 cm in length referred to as one-meter core drill. The present work is measured by the indirect method (Palmstrom, 2005) by counting parts more than 10 cm referred to one-meter stick as a percentage number.
3. Joint or discontinuity spacing: as the average measure between two successive joints in the same set in metric units.
4. Joint condition parameters include persistence, aperture, infillings, weathering condition, roughness, and waviness.
5. Groundwater condition is the condition of groundwater inflow in liters per minute. The studied locations are almost completely dry.

The total rating is calculated by summing up all of the above-mentioned parameters rates to get the RMR basic total for each site location. RMR

values for a given engineering structure are: very good (RMR 100–81), good (80–61), fair (60–41), poor (40–21), and very poor (20).

#### IV-2. Slope Mass Rating (SMR):

Romana (1985) and modified by Romana et al. (2003 and 2015) suggested this classification system for assessing the stability of rock slopes and is applied in the present study. SMR is calculated by adding adjustment factors for the relationship between the joint and slope and adding a factor based on the method of excavation from Bieniawski's rock mass rating (RMR).

$$SMR = RMR_{basic} + (F1, F2, F3) + F4$$

Where;

F1 depends on the parallelism between discontinuity dip direction,  $\alpha_j$ , and slope dip,  $\alpha_s$ . The empirical equation of F1 is  $F1 = (1 - \sin A)$ , A is the angle between Joint and slope dip directions.

F2 depends on the joint dip angle ( $\beta_j$ ), where  $F2 = \tan(\beta_j)$ . In planar failure mode, the dip of the critical joint is less than 20 degrees and less critical when joints dip more than 45°. F2 equal to 1 in toppling failure mode.

F3 depends on the relation between slope face and joint dip. In planar failure F3 depends on daylighting of critical joints on the slope face ( $\beta_j - \beta_s$ ), where  $\beta_j$  is the dip of joint and  $\beta_s$  is the dip of slope face. In wedge failure mode,  $F3 = \beta_j - \beta_s$ , where  $\beta_i$  is the plunge of the line of intersection between the two conjugate joints. It is fair condition when the slope face and joint face are parallel and unfavorable as slope dips  $\beta_j$  more than joint dip (in planar failure) and plunge of intersection line between conjugate joints (in wedge failure). For toppling failure, it depends on the sum of dips of slope face and joint dip ( $\beta_j + \beta_s$ ).

F4 depends on the adjustments of the excavation method, while F1, F2, F3 are factors controlled by the difference in joint orientation.

Romana (1985) and Romana et al. (2003 and 2015) indicated five stability classes for the SMR rating values as follows:

Class I: SMR = 100–81, Very good, completely stable, failure probability = 0,

Class II: SMR = 80–61, Good, stable, failure probability = 0.2,

Class III: SMR = 60–41, Normal, partially stable, failure probability = 0.4,

Class IV: SMR = 40–21, Bad, unstable, failure probability = 0.6, and

Class V: SMR = 20–0, Very bad, completely unstable, failure probability = 0.9.

### IV-3. Kinematic studies

Finally, kinematic studies are done on the joints and slope faces data collected from the chosen stations using DIPS v.7.0 software (Rocscience Inc., 2020), where possible failure type (planar, wedge, and toppling) is determined, as well as, the most critical failure surface in the rock slope is identified.

The rock exposures at stations 3 and 5 show considerable probability for wedge failure. Fracture orientations and their roughness condition and also slope face attitude for these stations are used in Swedge v 7.0 software (Rocscience Inc., 2021) to analyze wedge failure and computing volumes, weights, and estimated safety factor for the potential wedge block failure.

### V- Rock Mass Classification results of studied locations:

All studied locations are occupied by limestone of early Eocene age, which is the foundation rock of the new city and the cuts through the

highway road. It varies lithologically from more dolomitic limestone in stations S1 and S3 to less dolomitic chalky karstic limestone in S2, S4, and S5. The results of the evaluation of the RMR and RSR of the rocks in the chosen stations are listed in Tables 1 & 2, respectively. Table 3 shows the probability of failure for these locations.

#### V-1. Rock Mass Rating system (RMR):

The results of RMR basic in the RMR quality classification show that stations within the Galala city (S4 and S5) are good and upper fair, respectively, while S1, S2, and S3 give Fair rock quality (Tables 1 & 3).

The road cuts along the highway at stations S1, S2 and S3 have RMR values ranging between 47-53 and are classified as Class III while S4 and S5 have RMR values 58-63 to give Class II.

From the RMR values for stations within Galala city rock cuts, we can assume from its rock grade that it gives allowable bearing pressure about 440 – 280 (T/m<sup>2</sup>).

TABLE 1. RMR rock classification in the chosen stations.

Rock Mass Rating RMR Parameter	S1		S2		S3		S4		S5	
	Deg. / No.	R	Deg. / No.	R	Deg. / No.	R	Deg. / No.	R	Deg. / No.	R
1- Rock Strength UCS in (Mpa)	42.95	4	24.49	2	45.6	4	26.72	4	23.94	2
2- Rock Quality Designation (RQD)	40-60%	8	40-50%	8	30-40%	8	70%	13	50 -55%	13
3-Spacing between adjacent Discontinuities	J2 (9cm)	8	J3 (60cm)	15	J2 (10 cm)	8	40cm	10	J3 (40cm)	10
4-Discontinuity Condition										
· Persistence	>20m	0	5m	2	3-10m	2	1-3m	4	>20m	0
· Aperture	1mm	4	10-20mm	0	2-5mm	1	2-5mm	1	1-2mm	4
· Roughness	Rough	5	S. Rough	3	Sliken.	0	Rough	5	Rough	5
· Infillings	no fill	6	no fill	6	no fill	6	no fill	6	no fill	6
· Weathering	M. weather.	3	H. weather.	1	M. weather.	3	S. weather.	5	M. weather	3
5- Groundwater Condition	C. Dry	15	Damp	10	C. Dry	15	C. Dry	15	C. Dry	15
Total RMR	Fair	53	Fair	47	Fair	47	Good	63	Fair	58

S. Rough = Slightly Rough, Sliken. = Slikensided, M. Weather. = Moderately Weathered, H. Weather. = Highly Weathered, S. Weather. = Slightly Weathered, C. Dry = Completely Dry.

**V-2. Slope Mass Rating system (SMR):**

The SMR is determined from the RMR value in each station as proposed by Romana (1985) and Romana et al. (2003 and 2015). The SMR factors are computed for each measured joint set affecting the slope face. Among the calculated SMR ratings, the lowest value is considered as the representative rating value of the station.

The estimated SMR ratings indicate that Stations S1, S4, and S5 are of Normal quality while S2 and S3 are of bad quality (Tables 2&3).

The stability behavior, defined from the SMR values, indicates that S1, S4, and S5 are partially stable with a probability of failure 0.4, and S2 and S3 are unstable with a probability of failure 0.6 (Table 3).

**VI- Kinematic analysis results of studied locations**

DIPS 7.0 software was used to apply the kinematic studies on rock cuttings for structurally controlled failure in the studied sites. It gives results for the percentage of critical joint set planes or intersections able to failure and projection plots for every mode of failure in the studied stations (Table 4).

The analysis indicates planar failure in two stations (S2 and S5), where S2 has a lower percent than S5 (Table 4). S2 lies at about 800 m away from the asphaltic road and has no direct impact on the road course, meanwhile, S5 is more critical since it lies on a scarp bounding the city location at its northern boundary (Fig. 6).

**TABLE 2. SMR rock classification in the chosen stations.**

Factors of SMR:	S1		S2		S3		S4		S5	
	Deg. /No.	R	Deg. /No.	R	Deg. /No.	R	Deg. /No.	R	Deg. /No.	R
F1 ( $\alpha_j - \alpha_s$ ):	>30	0.15	20	0.7	<5	1	>30	0.15	>30	0.85
F2 ( $\beta_j$ or $\beta_i$ ):	>45	1	>45	1	25	0.4	>45	1	>45	1
F3 ( $\beta_j - \beta_s$ ):	-5	-50	-3	-50	-45	-60	>120	-25	>120	-25
F4:	NB	0	NS	15	NB	0	NB	0	NS	15
<b>Total RMR:</b>	53		47		47		63		58	
<b>Total SMR:</b>	46.5		27		23		59.25		51.75	

**TABLE 3. Shows the stations rock evaluation results RMR, SMR Stability, and Probability of failure.**

Classification/station	S1	S2	S3	S4	S5
<b>RMR Classification</b>	Fair	Fair	Fair	Good	Fair
<b>SMR Classification</b>	Normal	bad	bad	Normal	Normal
<b>Stability</b>	Partially Stable	Unstable	Unstable	Partially Stable	Partly Stable
<b>Probability of failure</b>	0.4	0.6	0.6	0.4	0.4

**TABLE 4. Percentages of critical joint failures in study stations.**

Station	S1	S2	S3	S4	S5
Planar failure (%)	0	15.7	0	0	26
Wedge Failure (%)	59.38	75.91	32.78	33.95	62.47
Toppling Failure (%)	4.82	15.71	0	0	30.67

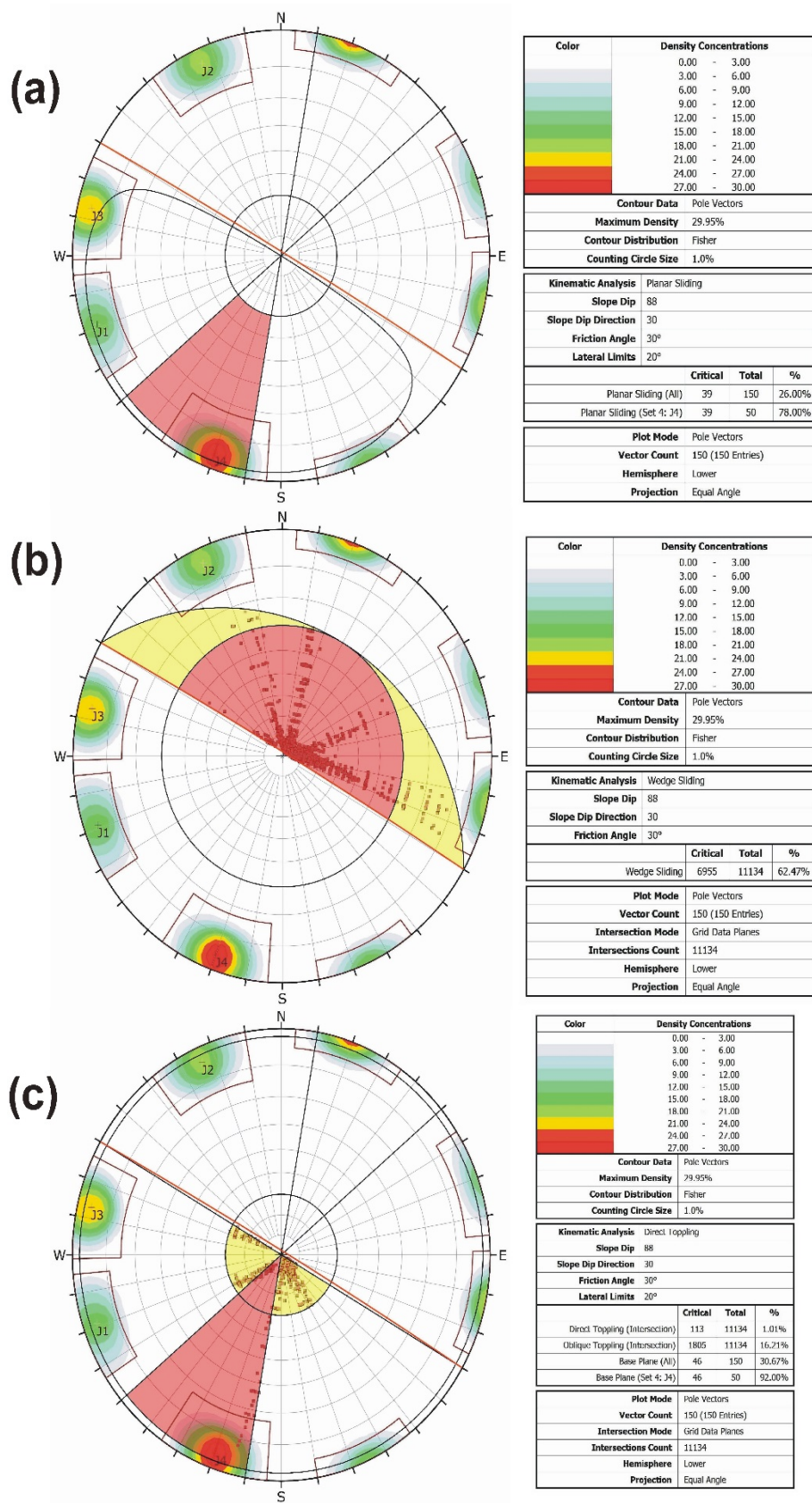


Fig. 6. Plateau cliff at station 5 bounding the city at its northern boundary showing sets of joints.

Wedge failure is susceptible in all stations where S3 and S5 have a significant potential to fail wedged block. S1 isn't critical because the elevation of the rock mass is lower than road and away from human activity. Also, S2 is not critical because it is distant from the asphaltic road.

The mechanism of toppling direct failure analysis shows the high potentiality of topples fall in S5 where there is a high cliff on Galala city borders.

### 1. Planar failure mode:

The analysis shows that S2 and S5 have the potentiality to planar failure with critical percentages (Table 4). The results of SMR classification as the probability of failure for S2 and S5 are 0.6 and 0.4 respectively. Planar failure in the S5 city cliff station is critical as there are many constructions are built along the city cliff.

The kinematic analysis of S5 for planar failure is shown in Fig. 7.a.

### 2. Wedge failure mode:

The results of SMR classification in S2 and S3 are unstable conditions (Table 3). Also, there are critical intersections present for wedge failure potentiality in all stations.

S5 shows a considerably high potentiality for wedge failure (62.47 %, table 4). The kinematics for wedge failure in this station indicates a large number of lines of intersections daylighting the slope (Fig. 7.b). The factor of safety under static condition calculated by Swedge software for six arbitrary chosen cases of these wedges is lower than unity and ranging between 0.453325 and 0.88023 (Table 5), indicating unsafe condition.



Fig. 7. Kinematic analysis of station 5. a) Plane failure potentiality. b) Wedge Failure Potentiality. Red points are critical intersections of joint planes daylighting slope. c) Toppling Failure Potentiality at S5.

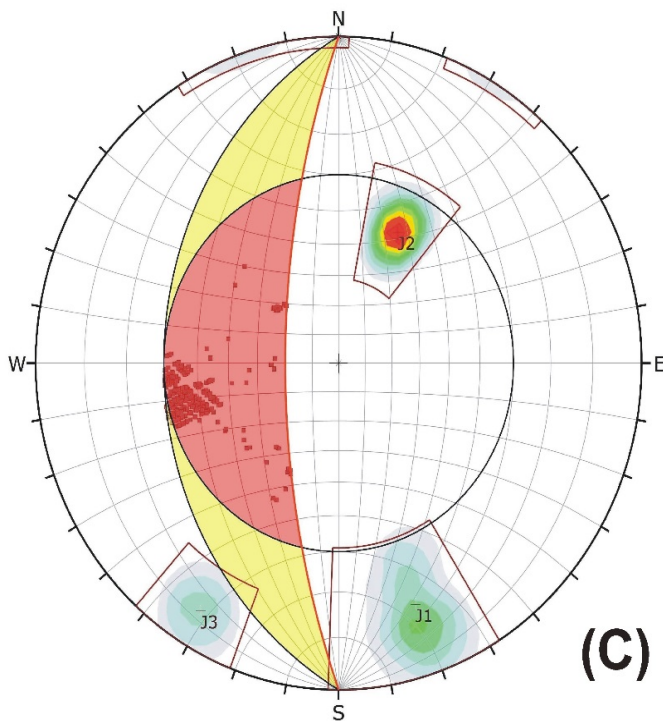
TABLE 5. Safety factor for six wedges in station 5.

Case	J1 & J2 (dip/ direction)	intersection (dip/ direction)	slope face (dip/ direction)	upper face (dip/ direction)	slope height (m)	Safety factor
1	87/065	85/011	88/030	5/030	200	0.532515
	85/020					
2	85/020	79/082	88/030	5/030	200	0.453325
	86/150					
3	87/015	80/088	88/030	5/030	200	0.761171
	87/160					
4	87/065	85/012	88/030	5/030	200	0.490042
	85/014					
5	86/100	84/052	88/030	5/030	200	0.555139
	85/020					
6	84/160	77/097	88/030	5/030	200	0.88023
	85/024					



(a)

(b)



(c)

Symbol	Feature
■	Critical Intersection

Color	Density Concentrations
	0.00 - 4.00
	4.00 - 8.00
	8.00 - 12.00
	12.00 - 16.00
	16.00 - 20.00
	20.00 - 24.00
	24.00 - 28.00
	28.00 - 32.00
	32.00 - 36.00
	36.00 - 40.00

Contour Data	Pole Vectors
Maximum Density	39.67%
Contour Distribution	Fisher
Counting Circle Size	1.0%

Kinematic Analysis	Wedge Sliding
Slope Dip	70
Slope Dip Direction	270
Friction Angle	30°

	Critical	Total	%
Wedge Sliding	417	1272	32.78%

Plot Mode	Pole Vectors
Vector Count	51 (51 Entries)
Intersection Mode	Grid Data Planes
Intersections Count	1272
Hemisphere	Lower
Projection	Equal Angle

Fig. 8. a. Potential Wedge failure in S3. b) Wedge rock failure fall. c) Kinematic analysis for joints in S3 showing wedge failure potentiality. Red points are critical intersections of joint planes daylighting slope.

In the S3 road cut section, a damaged zone of a minor fault of E-W trend is recorded where conjugate fractures of two main fracture orientations with opposite dip directions strike across the slope face forming wedge failures potential (Fig. 8. a & b).

The factor of safety of a rock wedge to slide rises significantly with the decreasing wedge angle for any given dip of the junction of its two joint planes (Hoek and Bray, 1981). The dip and dip directions for the studied potential failure planes J1 and J2 are 64/337 and 40/205, respectively, giving a line of intersection with plunge and trend 25/262 facing slope face on the highway roadcut of slope angle and slope direction 70/270 (Fig. 8. c). The estimated safety factor using Swedge deterministic analysis calculations is 2.0866 in static dry condition (Fig. 9), while in the most tragic dynamic condition as it is wet and influenced by seismic external forces this number reduced to 1.19, indicating acceptable safe condition.

### 3. Toppling failure mode:

In direct toppling failure, two joint sets intersect to create intersection lines dipping into the slope, which can form discrete blocks, while

the third set act as a release plane for the distinct block.

The toppling failure analysis shows that S2 and S5 have the potential for direct toppling failures (Table 4). Fig. 7.c shows the critical potentiality for toppling failure in S5 from the cliff at the northern city border.

### VII. Non-structurally controlled (karstification) failures:

It is well known that limestone rocks are usually affected by acidic groundwater to form surface and subsurface Karst caves, sinkholes, and increase the opening of fractures, which caused severe damage to buildings all over the world. These features resulted in many problems in buildings and roads in the new cities in Egypt constructed during the last decades.

From the field investigations in the study area, we found karstic limestone with numerous dissolution caves, cavities, and sinkholes in many locations (Fig. 10. a). Some stalactitic and stalagmitic features in cave openings on the highway road have been reported (Fig. 10. b). Infilling material in cavities and along fractures made up of clays and

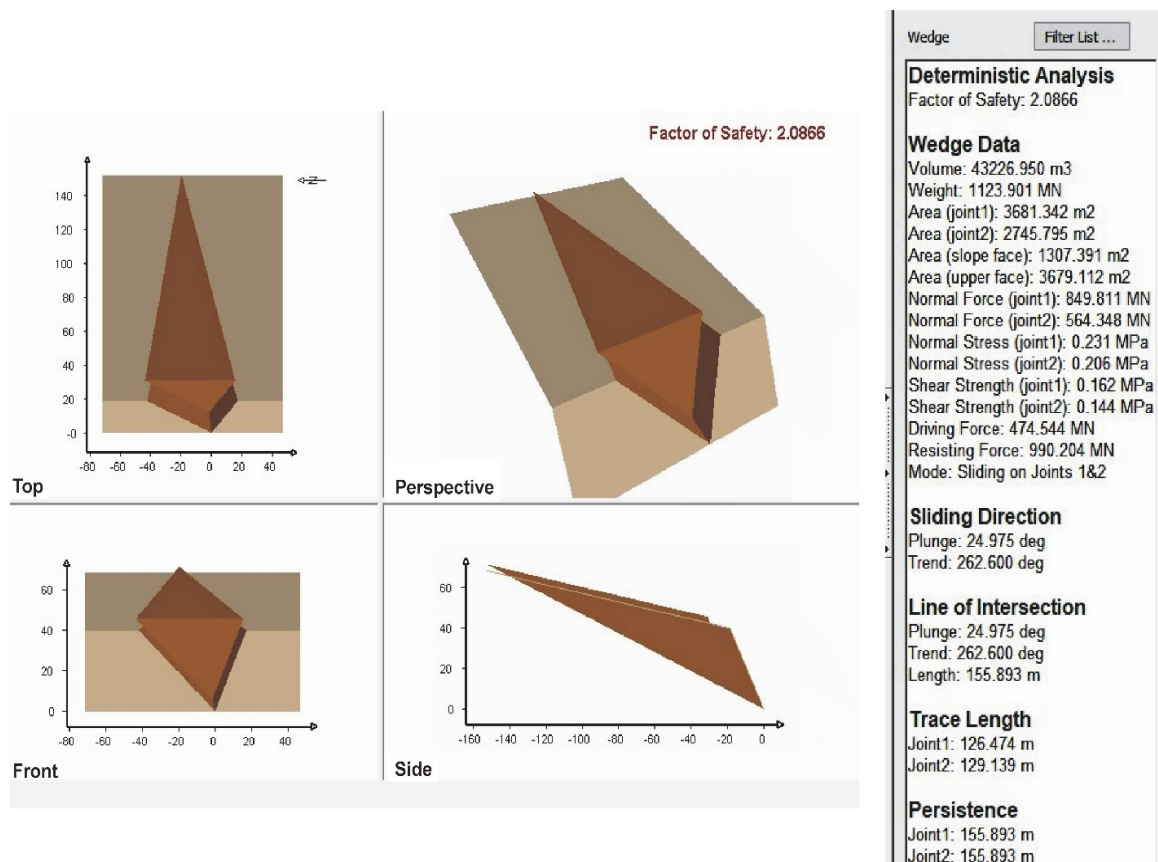
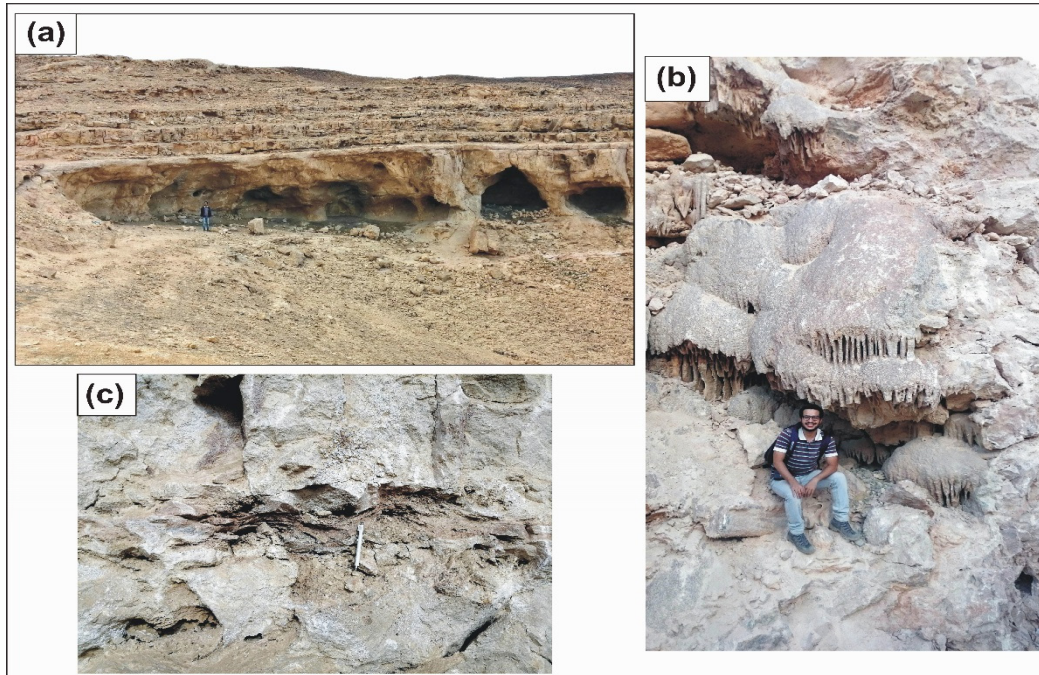


Fig. 9. Factor of safety calculation using Swedge software under static conditions in S3.



**Fig. 10. a. Caving and dissolution features recorded at station 2 nearby Galala city. b) Cave opening on the highway road showing sinkhole dissolution stalactites and stalagmites. c) Cavity filled with a soft secondary filling material.**

iron oxides are widely recorded (Fig. 10. c).

### **VIII. Conclusion**

The present study deals with the rock mass classification and evaluation of the rock quality and stability for the foundation of the new Galala City and the highway road leading to the city. The city location is situated on the Northern Galala Plateau that is covered mainly by the karstic Lower Eocene limestone. The study is accomplished through the determination of the RMR and SMR values and the kinematic analyses for five selected sites within the area.

In the study area the RMR values, in general, are ranging between 47 to 63, i.e., fair (Class III) to good (Class II); the SMR values range between 23 to 59.25, i.e., bad to normal; and partly stable.

Stations within Galala city show good (Class II) to fair (Class III) in RMR and Normal rock quality partly stable in SMR classification. This means a good foundation for urbanizing a new city with consideration of all precautions for the effect of the network of sewage and cultivation water and using ground insulators for cultivation areas to prevent groundwater dissipation from reaching the bedrock caves and joint network.

Stations along the asphaltic road where road

cutes are found show fair quality (Class III) in RMR, and bad in rock quality, and unstable in SMR classification.

Many different types of rock stability failure mechanisms are found in the study area as structurally controlled failures that are affected by Joints, faults, and discontinuities forming Planar, wedge, and toppling failures and also failures controlled by weathering and erosion effects in the form of Karst sinkholes, caves and cavities.

The kinematic analyses done on the chosen locations indicate two sites as most critical. The first is the scarp bounding the northern boundary of the city, where it has considerable potential for all types of failure (plane, wedge, and toppling), and proved to be unsafe for wedge failure with a safety factor lower than unity under static condition. The second is located along the asphaltic road, which shows a probable potentiality for wedge failure and considered to be safe with safety factor higher than unity under static and dynamic conditions.

The rock exposures in many locations within the study area are of cavernous limestone and have many dissolution caves and cavities. However, some of these locations show a good (class II) RMR, the presence of such karst features weakens the limestone in this horizon of lower Eocene and

must be taken into consideration.

For recommendations, the road cuts along the asphaltic road must be protected by a suitable protection method. Compacted engineering fill, engineering fill (using geosynthetic materials as reinforcement) concrete filling, and cement grout filling are four types of karstic limestone treatment. A suitable treatment type must be considered at the scarp present at the northern border of the city.

The hydrogeological and human urban water factors must be carefully studied and considered when evaluating potential failure problems already occurring and expected in the future, and in the future urban extension of the city. Karstic problems affect foundation rock strength as voids and cavities increase by groundwater percolation leading to widening and collapsing of these features. Sewage and cultivation water may represent serious future problems and must be taken into consideration.

Geophysical investigation studies based on GPR geophysical techniques is of prime importance and should be put into consideration to determine the subsurface Karst features in the foundation bedrock of the city location.

#### References

- Abdallah, M. A., Abd El-Hady, F. M. (1966): Geology of Sadat area, Gulf of Suez. *Egy. J. of Geo.* **10**, 1, 1-24.
- Abdallah, A. M., Adindani, A. (1963) Stratigraphy of Upper Palaeozoic rocks, western side of the Gulf of Suez. *Geo. Sur. of Egy.* **25**, 1-18.
- Abdallah, A.M., Adindani, A., Fahmy, N. (1963) Stratigraphy of the Lower Mesozoic rocks, western side of the Gulf of Suez. *Geo. Sur. of Egy.* **27**, 1-23
- Abd El-Aal, A. K., Masoud, A. A. (2017) Impacts of Karst Phenomena on Engineering Properties of Limestone Foundation Bed, Ar Riyadh, Saudi Arabia. *Arab. J. of Geosci.* **10**, 347, DOI 10.1007/s12517-017-3089-7
- Abdelazeem, M., Fathy, M. S., Khalifa, M. M. (2019) Integrating magnetic and stratigraphic data to delineate the subsurface features in and around new Galala City, Northern Galala Plateau, Egypt. *NRIAG J. of Astro. & Geophy.* **8**, 1, 131-143
- Abdeltawab, S., Ibrahim H. A. M. (1991) Unfavorable Geologic Setting of the New Minia City, Upper Egypt", *J. of Eng. and App. Sci., Cairo Uni.* **39**, 421 – 429.
- Abdeltawab, S. (1994) A Geotechnical Evaluation of El-Minia - Maghagha Area, Upper Egypt, *J. of King Abdul. Uni, Earth Sci.* **7**, 143-157.
- Abdeltawab, S. (2013) Karst limestone foundation geotechnical problems, detection and treatment: Case studies from Egypt and Saudi Arabia, *Inter. J. of Sci. & Eng.* **4**, 5, 376-387.
- Abdel Wahed, M., Fayed, L.A., Refaie, A. (2007) Structural and GPR studies on Beni-Suef El Gededa City: Structural and environmental hazards. *5th Inter. Conf. on the Geo. of Africa* **1**, IV- 1 - IV- 23.
- Adams, F. T., Lovell. C.W. (1984) Geotechnical Engineering Problems in the Karst Region of Southern Indiana. Joint Highway Research Project Report No. 84-12, School of Civil Engineering Indiana, Depart. of Highways, Purdue Uni., Indiana.
- Bandel, K., Kuss, J. (1987) Depositional environment of the pre-rift sediments of the Galala Heights (Gulf of Suez, Egypt). *Berliner geowissenschaftliche Abhandlungen (A)* **78**, 1-48.
- Basahel, H., Mitri, H. (2017) Application of Rock Mass Classification Systems to Rock Slope Stability Assessment: A Case Study. *J. of Rock Mech. and Geotech. Eng.* **9**, 6, 993-1009. DOI: 10.1016/j.jrmge.2017.07.007.
- Barton, N. R. (1979) Suggested Methods for the Quantitative Description of Discontinuities in Rock Masses. *Inter. J. of Rock Mech. and Min. Sci & Geomech. Abstracts* **16**, 2:22. DOI: 10.1016/0148-9062(79)91476-1.
- Boukhary, M., Kenawy A., Basta R. (2009) Early Eocene Nummulitids from Gebel Umm Russeies, El Galala El Bahariya, Eastern Desert, Egypt. *Geo. Croat.* **62**, 1, 1-18.
- Bieniawski, Z. T. (1973) Engineering classification of jointed rock masses. *Transact. of South African Instit. of Civil Eng.*, **15**, 12, 335-344.
- Bieniawski, Z.T. (1978) Geomechanics classification of rock masses and its application in tunneling. *Proc. Third Int. Cong. on Rock Mech.*, ISRM, Denver 1974, 27-32.
- Bieniawski, Z.T. (1989) Engineering rock mass classifications. John Wiley & Sons, New York, 251.
- CONOCO (1987) Geological map of Egypt 1:500,000, Beni Suef Sheet. The Egyptian General Petroleum Corporation.
- Darwish, M. (1992) Facies environments of the Upper Palaeozoic-Lower Cretaceous sequence in the Northern Galala Plateau and evidences for their hydrocarbon reservoir potentiality, Northern Gulf

- of Suez, Egypt. *Proceedings of the 1st Inter. Conf. Geo. Arab World, Cairo Univ., Cairo II*, 175–214.
- Deere, D.U. (1968) Geological considerations. *Rock Mechanics in Engineering Practice*, eds. K.G. Stagg and O.C. Zienkiewicz. John Wiley & Sons, London, 1-20.
- El-Haddad, B. A., Youssef A. M., El-Shater, A., El-Khashab, M. H. (2021) Landslide Mechanisms along Carbonate Rock Cliffs and Their Impact on Sustainable Development: A Case Study, Egypt. *Arab. J. of Geosci.* **14**, 7, 1–14. DOI: 10.1007/s12517-021-06688-1.
- El-Qot, G. M., Abdel-Gawad, G. I., Mekawy, M. S. (2009) Taphonomy of Middle Jurassic (Bathonian) Shell Concentrations from Ras El Abd, West Gulf of Suez, Egypt. *J. of Afri. Earth Sci.* **54**, 1–2, 31–36. DOI: 10.1016/j.jafrearsci.2009.03.002.
- Hammed M.S., Abdelkhalik A. (2015) 3D Digital Geological Mapping and Lithological Characterization of the Northwestern margin of the Gulf of Suez, Egypt by Integration of Remote sensing data, *15<sup>th</sup> inter. Multidisp. Sci. GeoConf. SGEM 2015*, Bulgaria, June 16-25, 2015
- Hoek, E., Bray, J.W. (1981) *Rock Slope Engineering*. Revised 3rd Edition, The Institution of Mining and Metallurgy, London, 341-351.
- Keheila, E. A. (2000) The impact of the Syrian arc system on carbonate facies stratigraphy and paleogeography of the lower Eocene northeastern desert, Egypt. *Egypt. J. of Geo.* **44**, 2, 147–82.
- Kuss, J., Scheibner, C., Gietl, R. (2000) Carbonate Platform to Basin Transition along an Upper Cretaceous to Lower Tertiary Syrian Arc Uplift, Galala Plateaus, Eastern Desert of Egypt. *GeoArab.* **5**, 3, 405–24.
- Mohammed, M. A., Abudeif A. M., Abd el-aal. A. K. (2020) Engineering Geotechnical Evaluation of Soil for Foundation Purposes Using Shallow Seismic Refraction and MASW in 15th Mayo, Egypt. *J. of Afri. Earth Sci.* **162**, 103721. DOI: 10.1016/j.jafrearsci.2019.103721.
- Moustafa, A. R., Khalil. M. H. (1995) Superposed Deformation in the Northern Suez Rift, Egypt: Relevance To Hydrocarbons Exploration. *J. of Petro. Geo.* **18**, 3, 245–66. DOI: 10.1111/j.1747-5457.1995.tb00905.x.
- Moustafa, A. R., Khalil S. M. (2020) Structure setting and tectonic evolution of the Gulf of Suez, NW Red Sea and Gulf of Aqaba rift systems, Chapter 8, 295-342, in Hamimi, Z. et al. (eds), *The Geology of Egypt, Regional geology Reviews*, Springer Nature Switzerland AG.
- Ogila, W.M.A., Abdel Tawab, S., Abdelkader, A.M., and Yousef, M. (2021) Analysis of Slope Stability Hazards along Hilly Highways: Ain Sukhna-Zafarana Highway, North Galala Plateau, Eastern Desert, Egypt. *Egypt. J. of Pure and App. Sci.* **59**(2):15–35. doi: 10.21608/ejaps.2022.107787.1013.
- Palmstrom, A. (2005) Measurements of and Correlations between Block Size and Rock Quality Designation (RQD). *Tunnel. & Undergro. Space Tech.* **20**, 4, 362–77. DOI: 10.1016/j.tust.2005.01.005.
- Rocscience (2020) DIPS v7.0 Graphical and Statistical Analysis of Orientation Data. Rocscience Inc., Toronto, Ontario.
- Rocscience (2021) SWEDGE v7.0 3D surface wedge analysis for slopes. Rocscience Inc., Toronto, Ontario.
- Romana, M. (1985) New adjustment ratings for application of Bieniawski classification to slopes, in: *Proceedings of the International Symposium on the Role of Rock Mechanics in Excavations for Mining and Civil Works. Inter. Soc. of Rock Mech., Zacatecas*, 49-53.
- Romana, M., Serón J. B., Enrique M. (2003) SMR Geomechanics Classification: Application, Experience and Validation. *10th ISRM Congr.* 4 (iii), 981–84.
- Romana, M., Tomás, R., Serón, J.B. (2015) Slope Mass Rating (SMR) Geomechanics Classification: Thirty Years Review. *13th ISRM Inter. Cong. of Rock Mech.* 1–10.
- Saada, S. A. (2016) Edge detection and depth estimation of Galala El Bahariya Plateau, Eastern Desert-Egypt, from aeromagnetic data. *Geomech Geophys Geo-Energy and Geo-Resour.* **2**, 1, 25–41.
- Scheibner, C., Marzouk, A. M., Kuss, J. (2001) Maastrichtian-Early Eocene Litho-Biostratigraphy and Palaeogeography of the Northern Gulf of Suez region, Egypt. *J. of Afr Earth Sci.*, **32**, 2, 223-255.
- Singh, B., Goel, R. K. (2011) *Engineering Rock Mass Classification*. Elsevier.
- Wanas, H. A., Soliman, H. E. (2018) Permo-Triassic Qiseib Formation, Western Side of the Gulf of Suez, Egypt: A Link of Fluvial Facies with Sequence Stratigraphy. *J Geo Geophys.* **7**, 3, 333. DOI: 10.4172/2381-8719.1000333.

## تقسيم كتل الصخر للحجر الجيري الأيوسيني الكارستي بمدينة الجلالة الجديدة، هضبة الجلالة البحرية، خليج السويس، مصر

عمرو جودة إسماعيل عبدالجواد<sup>(١)</sup>، وليلى عبدالمجيد فايد<sup>(١)</sup>، ومحمد عبدالواحد سليمان<sup>(١)</sup>، وهشام محمد حلمي<sup>(٢)</sup>  
<sup>(١)</sup> قسم جيولوجيا، كلية العلوم، جامعة القاهرة، و<sup>(٢)</sup> قسم الهندسة الإنشائية، كلية الهندسة، جامعة عين شمس، مصر

تستهدف الحكومة المصرية إلى إنشاء تجمعات ومدن عمرانية جديدة حول القاهرة والظهير الصحراوي لعواصم المحافظات. وتقع معظم هذه المدن الجديدة التي تم إنشائها على هضبة الأيوسين المكونة من الحجر الجيري الكارستي. وتعتبر مدينة الجلالة واحدة من هذه المدن الجديدة المنشأة على هضبة الجلالة البحرية. ولذا يحتاج موقعها إلى دراسات جيومرفولوجية وجيولوجية وجيوتقنية لتجنب المشاكل المستقبلية قبل الإشغال التام للمدينة. ويركز هذا البحث على دراسات مواقع حقلية لتقسيم كتلة الصخر (Rock mass Classification) وتقييم جودة وثبات الصخور بمدينة الجلالة وطريق الجلالة الذي يقطع صخور الأيوسين السفلى الجيرية الكارستية بهضبة الجلالة البحرية.

وخلال الدراسات الحقلية لتحديد مواقع الضعف بالهضبة من فوالق وفواصل وظواهر كارستية تم اختيار خمس مواقع دراسات حقلية، حيث تم تحديد اتجاهات والتعرف على صفات الفواصل لتقييم أسطح عدم الاتصال بها وتقسيم الكتل الصخرية (RMR) وتصنيف انحدار الكتل (SMR) والتحليل الحركي للصخور (Kine-matic Analysis) لتحديد أنماط الانهيار بالمواقع المختارة. وناقش البحث سبل تجنب تأثير عوامل التوسع العمراني من إنشاءات وطرق مقامة على صخور هضبة الجلالة بعد الإشغال التام للمدينة.